

## Supporting Information

## InP Quantum Dot-Organosilicon Nanocomposites

Mai Xuan Dung, Priyaranjan Mohapatra, Jin-Kyu Choi, Jin-Hyeok Kim,<sup>†</sup> Sohee Jeong,<sup>‡</sup> and Hyun-Dam Jeong<sup>\*</sup>*Department of Chemistry, Chonnam National University, Gwangju 500-757, Korea. \*E-mail: hdjeong@chonnam.ac.kr**<sup>†</sup>Department of Material Science and Engineering, Chonnam National University, Gwangju 500-757, Korea**<sup>‡</sup>Nanomechanical Systems Research Division, Korea Institute of Machinery and Materials, Daejeon 305-343, Korea**Received October 22, 2011, Accepted February 1, 2012***Synthesis of 3-aminopropyldimethylsilane (APDMS)**

Under a nitrogen atmosphere, 20.2 g (0.53 mol) of LiAlH<sub>4</sub> (95%, Aldrich) and 1.2 L of anhydrous diethylether (Aldrich) were loaded into a 2 L 2 neck flask. At 0 °C, 300 g (1.86 mol) of 3-aminopropyl dimethylethoxysilane (JSI Silicone, Seongam, South Korea) was added dropwise over 5 hours and the reaction was performed for 15 hours. The reaction mixture was then filtered to remove the solids and the filtrate was rotary evaporated at room temperature to obtain the products. Fractional distillation was conducted to collect about 10.3 g of APDMS (bp 127-131 °C) (4.7%). The product contained 70% of APDMS and 30% of a side-product (2,2-dimethyl-1,2-azasilolidine), as deduced from GC-MS and <sup>1</sup>H-NMR data in Figure S1.

**Testing the compatibility of the InP QDs and nanocomposite with the silicone encapsulant**

**Physical Mixing or Solvent Mixing.** In this process, QDs and silicon encapsulant were dissolved in a co-solvent such as toluene, or tetrahydrofuran to obtain a homogeneous solution which was then transferred to a glass slice for solvent evaporation gradually. As solvent evaporated, phase separation was obviously observed in all cases.

**InP-MA and Silicone Encapsulant.** 0.5 g of silicone encapsulant part B (6630B, Dow Corning) containing vinyl terminated polyorganosiloxane was added to 2 mL of a toluene solution containing 0.010 g of InP-MA under stirring. These solutions were dropped onto glass slides which were then placed in front of an Olympus SZ61 microscope equipped with a CVC5220 CCD camera (Velcam). The phase behavior of the solution during the time the solvent was being evaporated was monitored. The pictures shown in the top row of Figure 3(a) in the main text were snapped at different times.

**InP-APDMS and Silicone Encapsulant.** 0.5 g of silicone encapsulant part B (6630B, Dow Corning) containing vinyl terminated polyorganosiloxane was added to 2 mL of a toluene solution containing 0.013 g of InP-APDMS under stirring. These solutions were dropped onto glass slides and the phase separation was monitored. The left hand side

picture in the middle row in Figure 3(a) in the main text was snapped after evaporation of solvent.

**InP QD-organosilicon Nanocomposite and Silicone Encapsulant.** The InP QD-organosilicon composite obtained after 5 hours of the reaction between the InP-APDMS and the DVMSE was also tested. 0.2 (g) of the silicone encapsulant part B (6630B, Dow Corning) and 0.006 (g) of InP-DVMSE nanocomposite were mixed in toluene. The solution was poured on a glass slice to observe the phase behavior, as described above. The picture on the left hand side in the bottom row in Figure 3(a) (main text) was snapped after the solvent evaporation.

**Chemical Mixing.** InP-APDMS QDs or InP-DVMSE nanocomposite and the silicone encapsulant (6630B Dow Corning) containing vinyl terminated polyorganosiloxane were dissolved in toluene to perform a homogeneous solution. Pt catalyst (Karstedt, 2 wt % in toluene) was added to start the hydrosilylation reaction. When the toluene was evaporated by exposing this solution to the ambient conditions, phase behaviors of the mixtures were observed by mean of microscopy, as presented above. In contrast to the physical mixing method, composite obtained by this way were homogeneous and transparent.

**InP-APDMS and Silicone Encapsulant.** 0.2 g of the silicone encapsulant (6630B, Dow Corning) was added to 1 ml of a toluene solution containing 0.01 (g) of the InP-APDMS under stirring. After 10 minutes, a drop of Karstedt catalyst solution (2 wt % in toluene) was added and the mixture was stirred strongly to disperse the Pt catalyst. The viscosity of the reaction solution increased and the mixture became a gel after about 30 minutes, confirming the reaction between the InP-APDMS QDs or InP QD-organosilicon composite and the silicone encapsulant. The gel was then pressed between two transparent glass slides in order to obtain microscopic picture of the InP QD – silicone encapsulant composite. The pictures shown in the middle row of Figure 3(a) (in the main text) was snapped after drying the toluene solvent.

**InP QD-organosilicon Nanocomposite and Silicone Encapsulant.** Under stirring, 0.2 g of the silicone encapsulant (6630B, Dow Corning) was added to 1 mL of a toluene solution containing 0.01 (g) of the InP QD – organosilicon

nanocomposite which had been obtained after 5 hours of hydrosilylation between the InP-APDMS QD and DVMSE. After 10 minutes, a drop of Karstedt catalyst solution (2 wt% in toluene) was added to start the hydrosilylation reaction. After 30 minutes of the reaction, the solution was poured on a glass slice for microscopic monitoring, as mentioned above. The picture on the right hand side of Figure 3(a) in the main text was snapped after drying of the toluene solvent.

### Theoretical Calculations

To support our assertion that the coordination of the higher-electron donating APDMS to the In atom on the QD surface makes the interaction between the In atom and the neighboring P atom weaker, resulting in weaker P passivation, and hence inducing more PL quenching, than when the relatively-lower-electron donating MA is coordinated to the In atom on the QD surface, theoretical calculations were carried out on a simple cluster model chemistry in Gaussian03.<sup>2</sup>

For the cluster model chemistry to describe the In-rich surface QD, the idealized  $\text{In}_7\text{P}_8$  structure was introduced, in which two side-by-side In dimers are attached to eight “bulk” P atoms and three “bulk” In atoms, with four “surface” In atoms,<sup>3</sup> as shown in the left hand side of the Figure 8 in the main text. Since InP has both of covalent and

dativ bond contributions (three covalent bonds and one dative bond for each In and P atom), it is not valid to terminate all of the truncated bulk bonds in the cluster just with hydrogen, which is the typical way for covalent materials such as silicon. A logical treatment for a dative bond is to leave it with remaining a pair of electrons in the P atom,<sup>3</sup> which is adopted to construct the InP cluster model used here. In the cluster model, five of bulk P atoms are terminated with a pair of electrons, respectively, while remaining three P atoms (second layer) and three In atoms (third layer) are truncated with hydrogen, maintaining tetra-coordination for all bulk In atoms. Although such a treatment might not be able to describe exact chemical situation, we believe that it would afford a model appropriate enough to compare the effects of different ligand molecules (MA and APDMS) on the cluster.

We considered two different situations that the ligand molecules (MA and APDMS) were coordinated on the cluster by approaching to one surface In atom (edge-type) and the center between two surface In atoms (center-type), respectively, in which the MA was assumed to dissociate from its neutral form, giving an additional hydrogen on the surface In atom. After coordination of the ligand molecules, the whole molecular structure was fully optimized at DFT-B3LYP level. The calculation results are summarized and presented in Table 2 and Figure 8 in the main text.

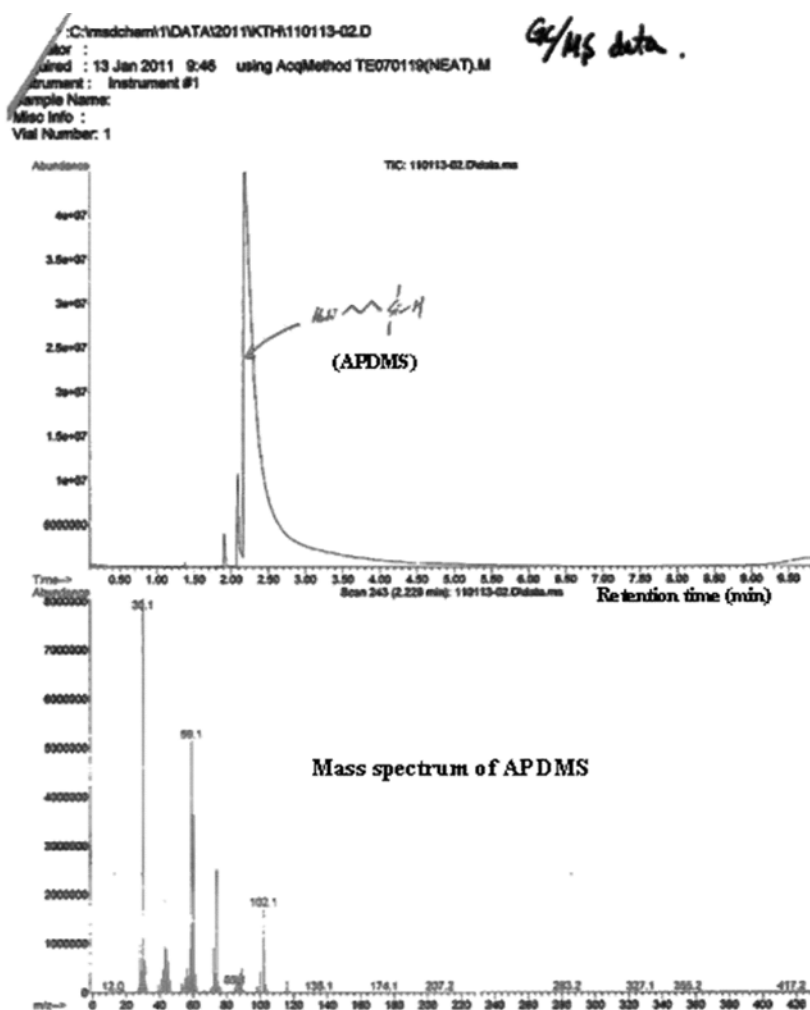


Figure S1. (a) GC-MS spectrum shows the formation of 3-aminopropyltrimethylsilane.

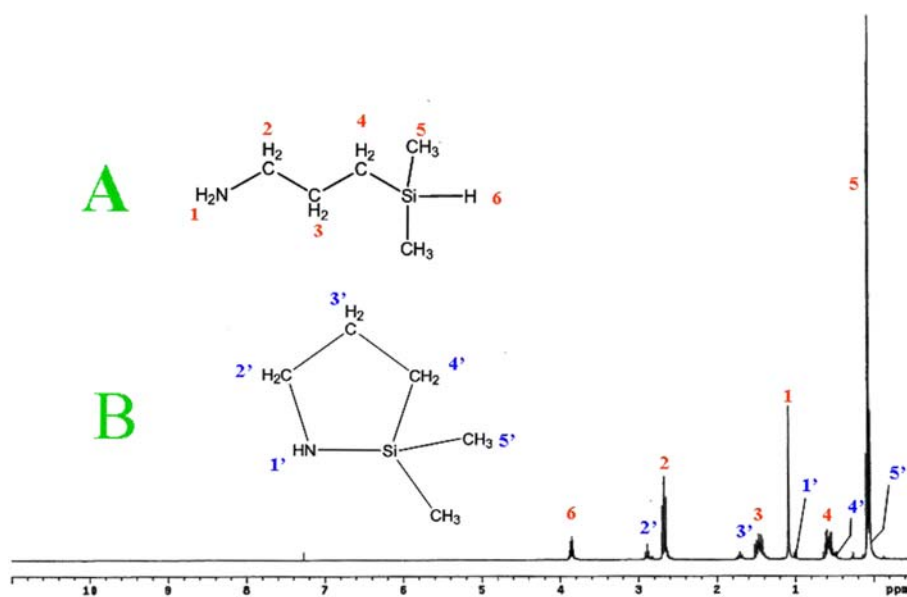
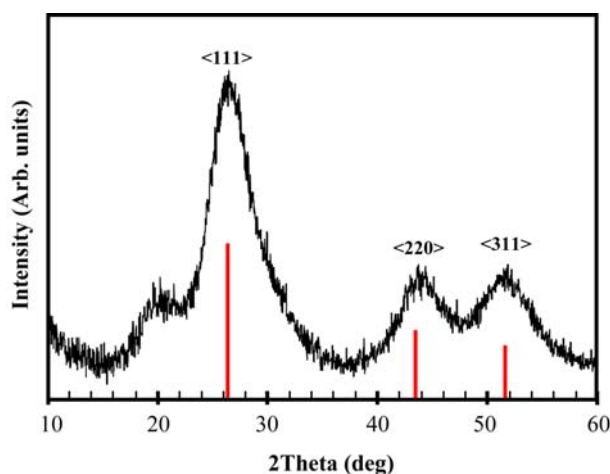


Figure S1. (b)  $^1\text{H-NMR}$  ( $\text{CDCl}_3$ ) spectrum of the 3-aminopropyltrimethylsilane (APDMS) ligand. Product contains by-product, 2,2-dimethyl-1-aza-2-silacyclopentane, labelled as **B**, with molar concentration of 30%.



**Figure S2.** (a) Wide angle X-ray diffraction pattern of the InP QDs.

The three peaks located at  $2\theta = 26.4^\circ$ ,  $43.8^\circ$  and  $51.8^\circ$  which are correlated with the three characteristic peaks of zinc-blende bulk InP crystal (red indicators) diffracted from the <111>, <220>, and <311> lattice planes, respectively, indicating the crystalline nature of the InP quantum dots.<sup>1</sup> The broadness of the peak in the XRD pattern is related to

the size of the InP crystal phase. Using the Scherrer equation:  $d = 0.9\lambda/\beta\cos\theta$  ( $d$ ,  $\lambda$ ,  $\beta$  and  $\theta$  are the diameter of the InP QDs, the X-ray wavelength of 0.154 nm, the FWHM in radians of the studied peak and the Bragg refracted angle, respectively), the size of the InP QDs was estimated to be 2.9 nm.

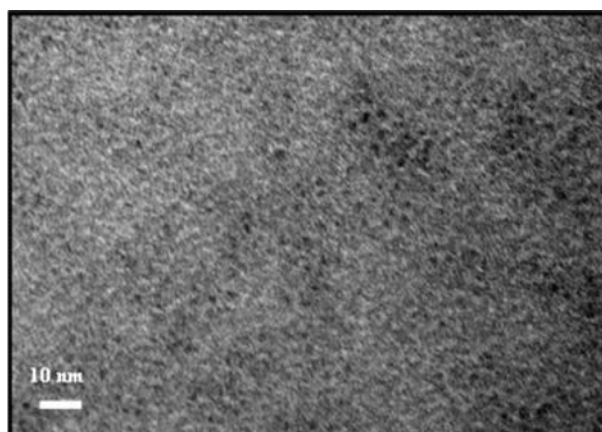


**Figure S2.** (b) TEM picture of the InP-MA quantum dot. The diameter of InP QD is about 3.6 nm as estimated from 36 dots

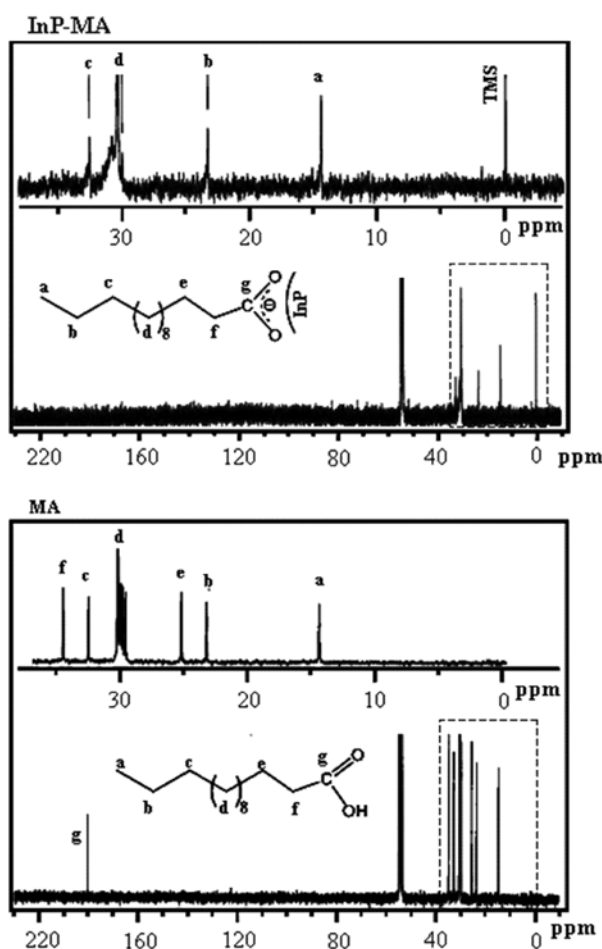


**Figure S3.**  $^{13}\text{C}$ -NMR spectra (in  $\text{CD}_2\text{Cl}_2$ ) of the commercial myristic acid (MA: below) and the MA capped InP QD (InP-MA: above). In each spectrum, the regions from  $-8$  to  $38$  ppm (dashed rectangles) are enlarged and shown above for clarity.

The lack of the three peaks originating from the carboxyl group and the two methylene groups next to the carboxyl moiety, referred to as **g**, **f** and **e** located at about  $180.0$ ,  $34.5$  and  $25.3$  ppm, respectively are due to the inhomogeneous distribution of the magnetic environments experienced by the carbon atoms near the surfaces of the quantum dots.<sup>4</sup> Since the ligands are coordinated to the QD surface at different atoms whose affinities with the ligand molecules are depending on their coordination number. A less passivated

atom will have higher affinity with or greater interaction with the ligand. Therefore, different ligand molecules experience different chemical environments, so that those atoms close to the quantum dot give NMR peaks at different positions. As a result, the NMR peaks of the atoms near the QD have broad shapes when the concentration of the studied sample is high enough and they often cannot be seen in the low concentration sample, as in our case.

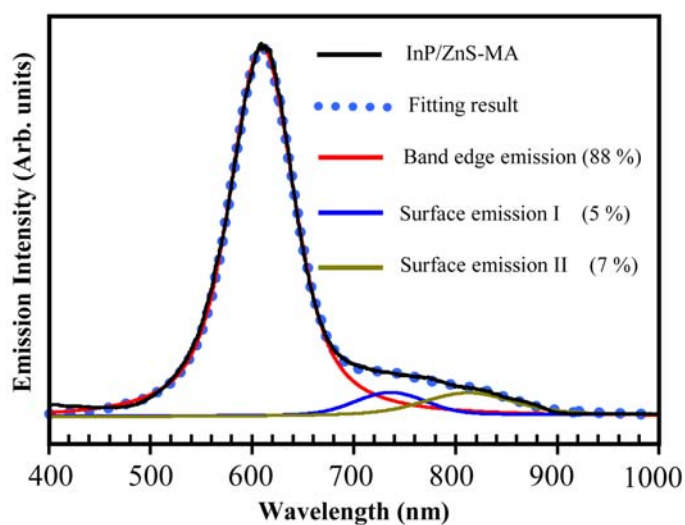


**Figure S4.** (a) Gaussian deconvoluted emission spectrum of the InP/ZnS-MA. Emission spectrum is well fitted by three components: band edge emission, surface emission I and II with relative contributions of 88%, 5% and 7%, respectively.

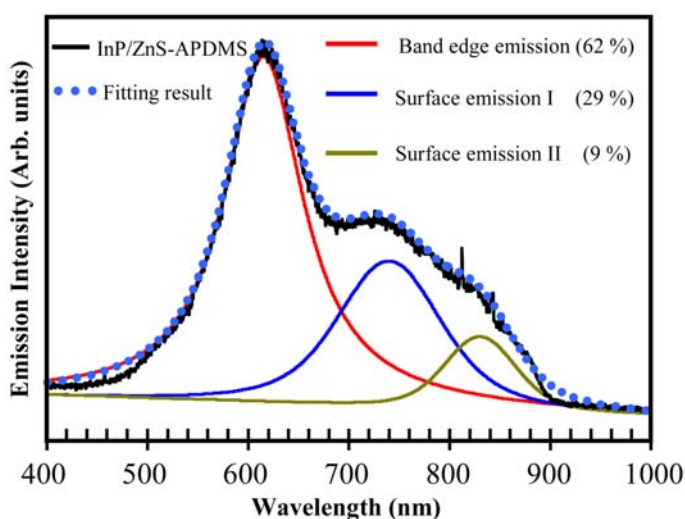


**Figure S4.** (b) Gaussian deconvoluted emission spectra of the InP/ZnS-APDMS. Emission spectrum is well fitted by three components: band edge emission, surface emission I and II with contributions of 62%, 29% and 9%, respectively.

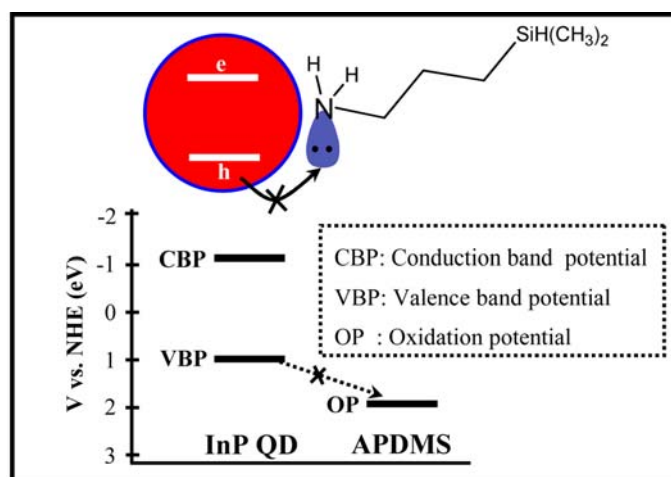


Figure S5. (a) Photoinduced hole transfer mechanism.

In this mechanism, a hole is expected to be transferred from the valence band of the quantum dot to the adsorbed amine molecule. This process is not allowed in our case, because the oxidation potential of APDMS is much higher than the valence band potential of the QDs. Herein, the valence band potential of the QDs is about 0.944 eV with

appropriate to that of the InP QD with a diameter of 3.6 nm reported by J. L. Blackburn.<sup>5</sup> Oxidation potential of APDMS is roughly equal to that of n-butylamine be 1.9 eV with respect to a NHE<sup>6</sup> because both molecules are primary, fatty amines and have a similar length.

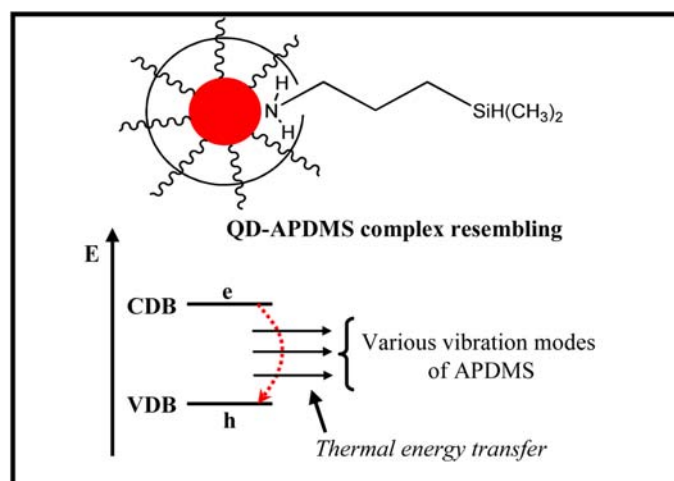
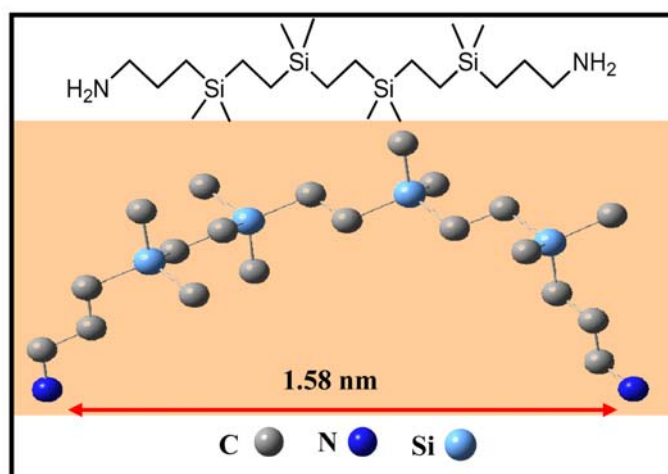


Figure S5. (b) Fast electron thermalization mechanism.

This mechanism explaining the PL quenching is based on the observation that the thermalization of the excited electron is speeded up by the adsorbed amine molecules on the surface of the QD.<sup>7</sup> The energy of the excited electron is transferred to the various vibration modes of the amine molecule. As a result, the exciton energy could be thermally extinguished in the QD – amine system in the same manner

as in a large molecular system,<sup>7</sup> where the emission wavelength is sure to be unchanged even after PL quenching. Therefore, we think that this mechanism cannot explain the red shifts in the emission spectrum observed in our cases either, as previously mentioned in Figure 5(a) and 6 in the main text.



**Figure S6.** Geometrically optimized structure of the linker constructed by two APDMS and one DVMSE molecules, using the Gaussian03 package at the B3LYP level and 6-31\*\* basic set.

#### Complete Author List of Reference 18a

Frisch, M. J.; Trucks, G. W.; Schlegel, H. B.; Scuseria, G. E.; Robb, M. A.; Cheeseman, J. R.; Montgomery, J. A., Jr.; Vreven, T.; Kudin, K. N.; Burant, J. C.; Millam, J. M.; Lyengar, S. S.; Tomasi, J.; Barone, V.; Mennucci, B.; Cossi, M.; Scalmani, G.; Rega, N.; Petersson, G. A.; Nakatsuji, H.; Hada, M.; Ehara, M.; Toyota, K.; Fukuda, R.; Hasegawa, J.; Ishida, M.; Nakajima, T.; Honda, Y.; Kitao, O.; Nakai, H.; Klene, M.; Li, X.; Knox, J. E.; Hratchian, H. P.; Cross, J. B.; Adamo, C.; Jaramillo, J.; Gomperts, R.; Stratmann, R. E.; Yazyev, O.; Austin, A. J.; Camml, R.; Pomelli, C.; Ochterski, J. W.; Ayala, P. Y.; Morokuma, K.; Voth, G. A.; Salvador, P.; Dannenberg, J. J.; Zakrzewski, V. G.; Dapprich, S.; Daniels, A. D.; Strain, M. C.; Farkas, O.; Malick, D. K.; Rabuck, A. D.; Raghavachari, K.; Foresman, J. B.; Ortiz, J. V.; Cui, Q.; Baboul, A. G.; Clifford, S.; Cioslowski, J.; Stefanov, B. B.; Liu, G.; Liashenko, A.; Piskorz, P.

Komaromi, I.; Martin, R. L.; Fox, D. J.; Keith, T.; Al-Laham, M. A.; Peng, C. Y.; Nanayakkara, A.; Challacombe, M.; Gill, P. M. W.; Johnson, B.; Chen, W.; Wong, M. W.; Gonzalez, C.; Pople, J. A. *Gaussian03*, RevisionD.1; Gaussian, Inc.: Wallingford, CT, 2005.

#### References

1. Battaglia, D.; Peng, X. *Nano Lett.* **2002**, 2, 1027.
2. Frisch, M. J.; *Gaussian03*; Gaussian, Inc.: Wallingford, CT, 2005.
3. Raghavachari, K.; Fu, Q.; Chen, G.; Li, L.; Li, C. H.; Law, D. C.; Hicks, R. F. *J. Am. Chem. Soc.* **2002**, 124, 15119.
4. Kuno, M.; Lee, J. K.; Dabbousi, B. O.; Mikulec, F. V.; Bawendi, M. G. *J. Chem. Phys.* **1997**, 106, 9869.
5. Blackburn, J. L.; Selmarten, D. C.; Ellingson, R. J.; Jones, M.; Micic, O.; Nozik, A. J. *J. Phys. Chem B* **2005**, 109, 2625.
6. Sharma, S. N.; Shurma, H.; Singh, G.; Shivaprasad, S. M. *Mater. Chem. Phys.* **2008**, 110, 471.
7. Darugar, Q.; Landes, C.; Link, S.; Schill, A.; El-Sayed, M. A. *Chem. Phys. Lett.* **2003**, 373, 284-291.